

## Article

# The Ongoing Deep Underground Measurement of $^{22}\text{Ne}(\alpha, n)^{25}\text{Mg}$ at the Ion Beam Facility of the INFN-LNGS

Andreas Best <sup>1,2,\*</sup> , David Rapagnani <sup>1,2</sup>  and Daniela Mercogliano <sup>1,2</sup> 

<sup>1</sup> Dipartimento di Fisica E. Pancini, Università di Napoli Federico II, Strada Comunale Cintia, 80126 Napoli, Italy

<sup>2</sup> INFN, Sezione di Napoli, Strada Comunale Cintia, 80126 Napoli, Italy

\* Correspondence: andreas.best@unina.it

**Abstract:** The  $^{22}\text{Ne}(\alpha, n)^{25}\text{Mg}$  reaction is of major importance in nuclear astrophysics. It is the main neutron source for the weak s-process and as such is responsible for the nucleosynthesis of  $60 < A < 90$  elements. In addition, it provides a strong neutron burst during the later, hottest phases of the main s-process, which modifies the final nucleosynthesis products, especially at so-called branch points, which can be used to provide insight into the stellar interior at that time. The reaction rate needs to be known below ca. 900 keV, and due to the low cross-section at these energies, a direct measurement has so far proven to be severely hampered by external neutron background at the surface of the Earth. To solve this problem, a measurement campaign (the ERC-funded SHADES project) was recently started at the deep underground Gran Sasso National Laboratory (LNGS) in Italy. We provide an overview of the experiment status and an outlook into the near future.

**Keywords:** nuclear astrophysics; deep underground laboratories; s-process; neutron detection



**Citation:** Best, A.; Rapagnani, D.; Mercogliano, D. The Ongoing Deep Underground Measurement of  $^{22}\text{Ne}(\alpha, n)^{25}\text{Mg}$  at the Ion Beam Facility of the INFN-LNGS. *Galaxies* **2024**, *12*, 68. <https://doi.org/10.3390/galaxies12060068>

Academic Editor: Dimitris M. Christodoulou

Received: 21 September 2024

Revised: 17 October 2024

Accepted: 22 October 2024

Published: 24 October 2024



**Copyright:** © 2024 by the authors. Licensee MDPI, Basel, Switzerland. This article is an open access article distributed under the terms and conditions of the Creative Commons Attribution (CC BY) license (<https://creativecommons.org/licenses/by/4.0/>).

## 1. Introduction

$^{22}\text{Ne}(\alpha, n)^{25}\text{Mg}$  is of crucial importance in various astrophysical nucleosynthesis scenarios: as the main neutron source of the weak s-process in massive stars, as a provider of a burst of neutrons in the late stages of the main s-process, and during the production of magnesium isotopes (see [1] and references therein).

The reaction has a negative Q value of  $-478.3$  keV [2], and its cross-section needs to be known as far down in energy as possible to provide the required input for astrophysical calculations. The expected cross-section is in the picobarn range and below, thus proving extremely challenging to measure in the laboratory. Direct attempts basically stopped over twenty years ago, after a measurement that through enormous effort was able to push down the extrinsic background level to about 100 cts/h, but was still unable to measure resonances in the crucial region below a strong resonance at  $E_{\alpha} = 832$  keV [3].

Instead, efforts have been focused on indirect measurements of resonance energies, spin-parities, and partial widths in order to calculate the contribution of low-energy states to the cross section. Significant improvements have been made, but many of the results are inconclusive or even contradictory, leading to large uncertainties in the astrophysical reaction rates [4–9].

To approach the problem through a direct measurement, the ERC-funded project “SHADES”<sup>1</sup> constructed a novel neutron detection array consisting of EJ-309 scintillators and  $^3\text{He}$  counters, a recirculating gas target and, most importantly, is locating the measurement in the deep-underground Gran Sasso National Laboratories, using the newly commissioned accelerator of the INFN Bellotti Ion Beam Facility (IBF) [10,11].  $^{22}\text{Ne}(\alpha, n)^{25}\text{Mg}$  is also part of the Laboratory for Underground Nuclear Astrophysics (LUNA) [12,13] collaboration scientific program, which plans to conclude the cross-section measurement by 2025. Together with ASFIN [14,15], n-TOF [16,17], ERNA [18–21], and PANDORA [22], LUNA is one of the main contributors to nuclear astrophysics research in Italy.

The combination of a high beam intensity, greatly suppressed neutron background, and the energy discrimination capabilities of the detector finally opens up the low-energy region to direct measurement. Where the last measurement attempt by Jaeger et al. [3] was limited in its sensitivity by the background count rate of over 100 cts/h, the already shown reduction in neutron background at the LNGS to below 2 cts/h [23,24] will allow for the probing of the most promising low-energy candidate states in the compound nucleus. In this paper, we present the current status of the project.

## 2. Experimental Setup

### 2.1. Gas Target

$^{22}\text{Ne}(\alpha, n)^{25}\text{Mg}$  will be measured as far down in energy as possible using a recirculated  $^{22}\text{Ne}$ -enriched extended gas target. Following Figure 1, through an aperture (A1, 7.5 mm diameter), the beam enters the first pumping stage, where a turbo-molecular pump<sup>2</sup> (TP1) is installed in differential configuration (i.e., it exhausts into another turbo-molecular pumping stage). A second aperture (A2, 7.5 mm diameter) is installed before a second pumping stage, again served by a turbo-molecular pump (TP2). A scroll pump<sup>3</sup> serves as a backing pump and is connected at the entrance of a high-volume Pfeiffer Vacuum A6-flow pumping one, which is located next to the reaction chamber and evacuated by the 604H pump. Two additional apertures (A4 and A5, both 6.0 mm diameter) separate the reaction chamber from the high-flow pumping stages. The last pumping stage is operated with another turbo-molecular pump (TP3) and is directly exhausted into the A604H pump. The beam is eventually stopped by a slab of water-cooled copper coated with tantalum ( $\sim 5 \mu\text{m}$ ). In a similar way, tantalum layers were installed in front of the apertures past the reaction chamber (tantalum thickness  $> 0.25 \text{ mm}$ ) and inside the internal surface ( $> 1 \text{ mm}$ ). A scroll pump operates at the outlet of the high-flow pump to perform the initial air evacuation. A bypass toward its inlet allows for a faster initial vacuum of the line. The same scroll pump is also used to exhaust the system buffer when no gas is present. A purifier just before the gas buffer entrance allows it to remove carbon contaminants (most relevant  $\text{CO}$ ,  $\text{CO}_2$ ,  $\text{CH}_4$ ). Finally, a gas flow controller between the buffer and the reaction chamber allows for a regulation of the neon to be injected. ISO-KF and ISO-F flanges are used, where the standard viton sealings are replaced with aluminium ones. They allow for a lower leak rate and avoid carbon degassing, which may cause the contamination of recirculating gas. Similarly, semiconductor industry-grade pumps are employed, which grant an enhanced isolation of the oiled components, if present, from the vacuum chambers. The whole vacuum system was operated remotely through a dedicated LabVIEW controller.

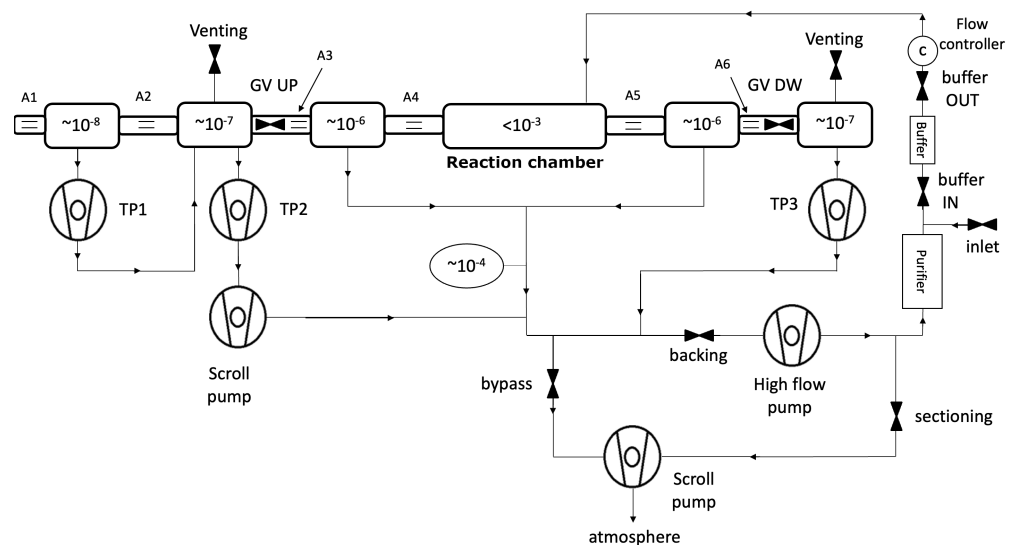


**Figure 1.** Schematic view of the  $^{22}\text{Ne}(\alpha, n)^{25}\text{Mg}$  beam line. The best vacuum levels reached without gas injection are reported. See the text for more details.

## 2.2. Detector Array

As stated above, the detector is a hybrid array consisting of 18  $^3\text{He}$  counters with a steel body and low intrinsic activity [25], and 12 EJ-309 organic scintillators ( $12 \times 12$  cm). They are connected to CAEN V1725 250 Msamples/s 14 bit digitisers and read out in synchronised clock mode in order to allow for coincidences between events. The scintillator has the advantage of a high flashpoint, thus allowing its safe introduction into the sensitive underground environment of the LNGS, while maintaining characteristics close to standard materials like NE213. Its intrinsic background has been characterised as part of the SHADES campaign and consists of the common contaminants in the aluminium body and radon emanation in the scintillator liquid [26]. The full setup is surrounded by a 2-inch-thick 5% borated polyethylene shielding that also acts as support structure for the detectors (for a view of the assembly see Figure 2).

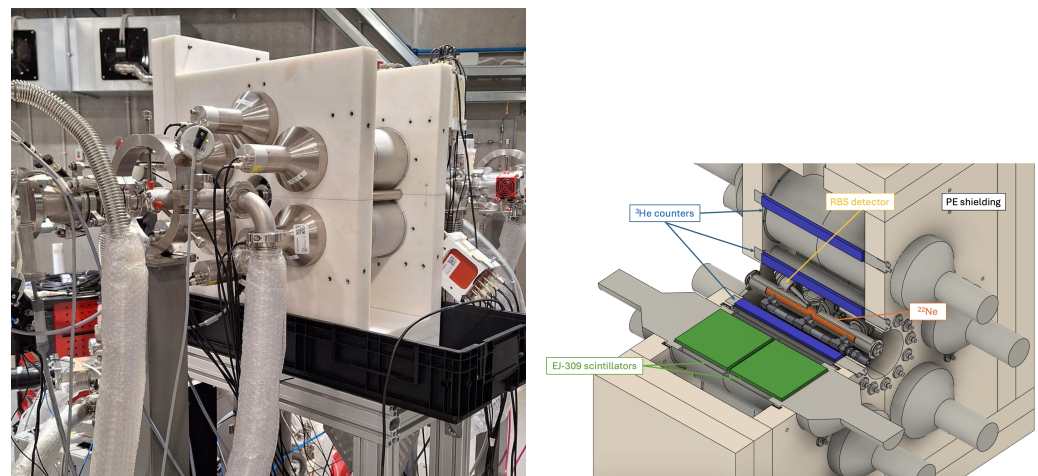


**Figure 2.** (Left) Partial SHADES detector array mounted around the recirculating gas target in the Bellotti IBF experimental hall. (Right) Schematic drawing of the detector array.

## 3. Preliminary Results and Status

Preliminary gas target tests show that a good vacuum level can be achieved, as shown from Table 1. At the first pumping stage, which acts as the interface with the beam line, a pressure as low as  $10^{-8}$  mbar can be achieved, which meets the requirements of the Bellotti IBF. An increase of one order of magnitude at each stage is measured, whereas a vacuum better than  $10^{-4}$  mbar is achieved in the reaction chamber, which is at the low end of the measurement range of the employed sensors. This estimate is sufficient, as the  $^{22}\text{Ne}$  injection pressure inside the reaction chamber is in the mbar range. Downstream of the gas target, from a lower pressure of about  $10^{-6}$  mbar a value of about  $10^{-7}$  mbar is reached at the latest pumping stage. When the  $^{22}\text{Ne}$  gas is injected at the estimated work pressure, i.e., up to 4 mbar, the vacuum level rise remains inside the IBF requirement.

**Table 1.** Best vacuum and pressure levels of SHADES gas target. The pressure inside the chamber ( $p_{\text{ch}}$ ), in the stages next to it ( $p_{\text{UP1}}$  and  $p_{\text{DW1}}$ ), in the turbo-molecular stages closer the reaction chamber ( $p_{\text{UP2}}$  and  $p_{\text{DW2}}$ , TP2 and TP3 in Figure 1), and in the first pumping stage ( $p_{\text{UP1}}$ , TP3) are reported.

$p_{\text{ch}}$	$p_{\text{UP1}}$	$p_{\text{DW1}}$	$p_{\text{UP2}}$	$p_{\text{DW2}}$	$p_{\text{UP3}}$	
$<1.0 \times 10^{-4}$	$5.8 \times 10^{-6}$	$6.5 \times 10^{-6}$	$1.1 \times 10^{-6}$	$8.5 \times 10^{-7}$	$8.6 \times 10^{-8}$	mbar
1.0	$6.8 \times 10^{-2}$	$6.8 \times 10^{-2}$	$5.7 \times 10^{-4}$	$4.8 \times 10^{-4}$	$7.3 \times 10^{-6}$	
2.1	$1.3 \times 10^{-1}$	$1.3 \times 10^{-1}$	$1.8 \times 10^{-3}$	$1.9 \times 10^{-3}$	$1.8 \times 10^{-5}$	
3.1	$1.6 \times 10^{-1}$	$1.6 \times 10^{-1}$	$3.5 \times 10^{-3}$	$2.7 \times 10^{-3}$	$2.7 \times 10^{-5}$	

The array has been taken into operation underground, and measurements with a neutron source and first alpha beam tests on natural neon were performed, whose data are under analysis. An example 2D Energy vs PSD histogram and coincidence timing between  $^3\text{He}$  counter and scintillator signals are shown in Figure 3. In this case, the discrimination parameter is based on the long-vs-short method  $\text{PSD} = \frac{I_L - I_S}{I_L}$ , where  $I_L$  is the integral over the entire pulse and proportional to the energy, and  $I_S$  is the integral over the rising part. The coincidence characteristics are currently under investigation.

Some beam-induced background was seen and located to the source from one of the gas target collimators, most likely caused by a straggled beam hitting a contaminated surface. The collimator was replaced and exposed surfaces were coated with gold.

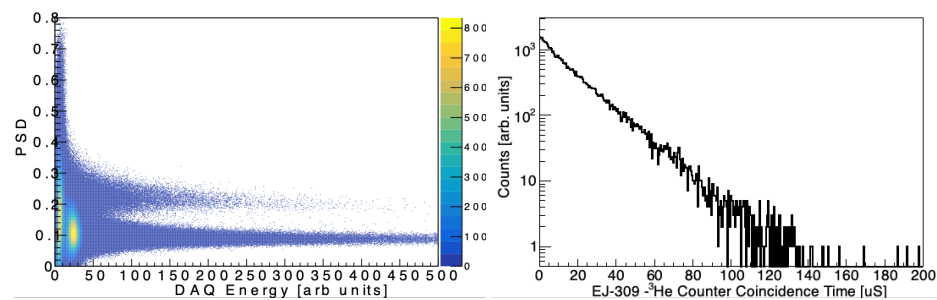


**Figure 3.** (Left) Example Energy vs. PSD histogram of the EJ-309 scintillators. Neutron signals fall in the PSD region above ca. 1.5, whereas photons lie in the band blue centred around  $\text{PSD} = 0.1$ . (Right) Coincidence time between neutron events gated on  $^3\text{He}$  counter signals.

#### 4. Outlook

After a maintenance shutdown of the MV accelerator, tests for beam-induced background were performed in late summer 2024, with promising preliminary results and a reduction in the background levels below those of Jaeger et al. A first long beam time for low-energy neutron measurements was foreseen for winter/spring 2024/2025. The 832 keV resonance will be repeatedly measured, to extract resonance energy, strength and possibly its width as well as reproducibility standard during the long low energy runs. Promising candidate states in the compound nucleus that have been identified in the indirect measurement campaigns will be focused on in order to improve the upper limits or, for the first time, measure their resonance strength. The underground campaign will conclude with efficiency measurements and a final characterisation of beam-heating effects and a gas target density profile. More efficiency measurements with reactions that are not possible underground are foreseen to take place in 2025, most likely at the ATOMKI laboratory in Debrecen, Hungary.

In conclusion, after more than 20 years, a new direct measurement campaign for the astrophysically important reaction  $^{22}\text{Ne}(\alpha, n)^{25}\text{Mg}$  has entered its production phase in the Bellotti IBF at the INFN-LNGS. Over the following year, it is expected that the experiment will drastically improve upper limits or measure low-energy resonance strengths that are crucial for astrophysical calculations in a variety of scenarios.

**Author Contributions:** Conceptualization, A.B.; methodology, A.B.; formal analysis, A.B., D.R., and D.M.; investigation, A.B., D.R., and D.M.; data curation, A.B., D.R., and D.M.; writing—original draft preparation, A.B. and D.R.; writing—review and editing, A.B., D.R., and D.M.; supervision, A.B.; project administration, A.B.; funding acquisition, A.B. All authors have read and agreed to the published version of the manuscript.

**Funding:** This work is supported by the European Union (ERC-StG 2019 SHADES #852016).

**Data Availability Statement:** The original contributions presented in the study are included in the article, further inquiries can be directed to the corresponding authors.

**Conflicts of Interest:** The authors declare no conflicts of interest.

## Notes

- <sup>1</sup> ERC-StG 2019 #852016, “Scintillator-<sup>3</sup>He Array for Deep-underground Experiments on the S-process”.
- <sup>2</sup> The three turbo-molecular pumps employed are Pfeiffer Vacuum HiPace 60.
- <sup>3</sup> The two scroll pumps employed are Pfeiffer Vacuum HiScroll 12.

## References

1. Adsley, P.; Battino, U.; Best, A.; Caciolli, A.; Guglielmetti, A.; Imbriani, G.; Jayatissa, H.; La Cognata, M.; Lamia, L.; Masha, E.; et al. Reevaluation of the  $^{22}\text{Ne}(\alpha, \gamma)^{26}\text{Mg}$  and  $^{22}\text{Ne}(\alpha, n)^{25}\text{Mg}$  reaction rates. *Phys. Rev. C* **2021**, *103*, 015805. [[CrossRef](#)]
2. Wang, M.; Huang, W.; Kondev, F.; Audi, G.; Naimi, S. The AME 2020 atomic mass evaluation (II). Tables, graphs and references\*. *Chin. Phys. C* **2021**, *45*, 030003. [[CrossRef](#)]
3. Jaeger, M.; Kunz, R.; Mayer, A.; Hammer, J.W.; Staudt, G.; Kratz, K.L.; Pfeiffer, B.  $^{22}\text{Ne}(\alpha, n)^{25}\text{Mg}$ : The Key Neutron Source in Massive Stars. *Phys. Rev. Lett.* **2001**, *87*, 202501. [[CrossRef](#)] [[PubMed](#)]
4. Wiescher, M.; deBoer, R.J.; Görres, J. The resonances in the  $^{22}\text{Ne}+\alpha$  fusion reactions). *Eur. Phys. J. A* **2023**, *59*, 11. [[CrossRef](#)]
5. Ota, S.; Christian, G.; Catford, W.N.; Lotay, G.; Pignatari, M.; Battino, U.; Bennett, E.A.; Dede, S.; Doherty, D.T.; Hallam, S.; et al. ( $^6\text{Li}, d$ ) and ( $^6\text{Li}, t$ ) reactions on  $^{22}\text{Ne}$  and implications for *s*-process nucleosynthesis. *Phys. Rev. C* **2021**, *104*, 055806. [[CrossRef](#)]
6. Adsley, P.; Brümmer, J.W.; Li, K.C.W.; Marín-Lámbarri, D.J.; Kheswa, N.Y.; Donaldson, L.M.; Neveling, R.; Papka, P.; Pellegrini, L.; Pesudo, V.; et al. Re-examining the  $^{26}\text{Mg}(\alpha, \alpha')^{26}\text{Mg}$  reaction: Probing astrophysically important states in  $^{26}\text{Mg}$ . *Phys. Rev. C* **2017**, *96*, 055802. [[CrossRef](#)]
7. Massimi, C.; Altstadt, S.; Andrzejewski, J.; Audouin, L.; Barbagallo, M.; Bécares, V.; Bečvář, F.; Belloni, F.; Berthoumieux, E.; Billowes, J.; et al. Neutron spectroscopy of  $^{26}\text{Mg}$  states: Constraining the stellar neutron source  $^{22}\text{Ne}(\alpha, n)^{25}\text{Mg}$ . *Phys. Lett. B* **2017**, *768*, 1–6. [[CrossRef](#)]
8. Talwar, R.; Adachi, T.; Berg, G.P.A.; Bin, L.; Bisterzo, S.; Couder, M.; deBoer, R.J.; Fang, X.; Fujita, H.; Fujita, Y.; et al. Probing astrophysically important states in the  $^{26}\text{Mg}$  nucleus to study neutron sources for the *s* process. *Phys. Rev. C* **2016**, *93*, 055803. [[CrossRef](#)]
9. Jayatissa, H.; Rogachev, G.; Goldberg, V.; Koshchiy, E.; Christian, G.; Hooker, J.; Ota, S.; Roeder, B.; Saastamoinen, A.; Trippella, O.; et al. Constraining the  $^{22}\text{Ne}(\alpha, \gamma)^{26}\text{Mg}$  and  $^{22}\text{Ne}(\alpha, n)^{25}\text{Mg}$  reaction rates using sub-Coulomb  $\alpha$ -transfer reactions. *Phys. Lett. B* **2020**, *802*, 135267. [[CrossRef](#)]
10. Sen, A.; Domínguez-Cañizares, G.; Podaru, N.; Mous, D.; Junker, M.; Imbriani, G.; Rigato, V. A high intensity, high stability 3.5 MV Singletron™ accelerator. *Nucl. Instrum. Methods Phys. Res. Sect. B Beam Interact. Mater. Atoms* **2019**, *450*, 390–395. [[CrossRef](#)]
11. Junker, M.; Imbriani, G.; Best, A.; Boeltzig, A.; Compagnucci, A.; Di Leva, A.; Ferraro, F.; Rapagnani, D.; Rigato, V. The deep underground Bellotti Ion Beam Facility—Status and perspectives. *Front. Phys.* **2023**, *11*, 1291113. [[CrossRef](#)]
12. Piatti, D.; Masha, E.; Aliotta, M.; Balibrea-Correa, J.; Barile, F.; Bemmerer, D.; Best, A.; Boeltzig, A.; Brogini, C.; Bruno, C.G.; et al. First direct limit on the 334 keV resonance strength in  $^{22}\text{Ne}(\alpha, \gamma)^{26}\text{Mg}$  reaction. *Eur. Phys. J. A* **2022**, *58*, 194. [[CrossRef](#)]
13. Skowronski, J.; Gesuè, R.M.; Boeltzig, A.; Ciani, G.F.; Piatti, D.; Rapagnani, D.; Aliotta, M.; Ananna, C.; Barile, F.; Bemmerer, D.; et al. Advances in radiative capture studies at LUNA with a segmented BGO detector. *J. Phys. Nucl. Phys.* **2023**, *50*, 045201. [[CrossRef](#)]
14. Spitaleri, C.; Cherubini, S.; La Cognata, M.; Lamia, L.; Mukhamedzhanov, A.; Pizzone, R.; Romano, S.; Sergi, M.; Tumino, A. Trojan Horse Method: Recent applications in nuclear astrophysics. *Nucl. Phys. A* **2010**, *834*, 639c–642c. [[CrossRef](#)]
15. Pizzone, R.; Spitaleri, C.; Cherubini, S.; La Cognata, M.; Lamia, L.; Romano, S.; Sergi, M.; Tumino, A.; Li, C.; Wen, Q.; et al. Trojan Horse Method: A useful tool for electron screening effect investigation. *Nucl. Phys. A* **2010**, *834*, 673c–675c. [[CrossRef](#)]
16. Borcea, C.; Cennini, P.; Dahlfors, M.; Ferrari, A.; Garcia-Muñoz, G.; Haefner, P.; Herrera-Martinez, A.; Kadi, Y.; Lacoste, V.; Radermacher, E.; et al. Results from the commissioning of the n\_TOF spallation neutron source at CERN. *Nucl. Instrum. Methods Phys. Res. Sect. A Accel. Spectrometers Detect. Assoc. Equip.* **2003**, *513*, 524–537. [[CrossRef](#)]
17. Esposito, R.; Calviani, M.; Aberle, O.; Barbagallo, M.; Cano-Ott, D.; Coiffet, T.; Colonna, N.; Domingo-Pardo, C.; Dragoni, F.; Franqueira Ximenes, R.; et al. Design of the third-generation lead-based neutron spallation target for the neutron time-of-flight facility at CERN. *Phys. Rev. Accel. Beams* **2021**, *24*, 093001. [[CrossRef](#)]
18. Buompane, R.; Di Leva, A.; Gialanella, L.; D’Onofrio, A.; De Cesare, M.; Duarte, J.; Fülöp, Z.; Gasques, L.; Gyürky, G.; Morales-Gallegos, L.; et al. Determination of the  $^7\text{Be}(p, \gamma)^8\text{B}$  cross section at astrophysical energies using a radioactive  $^7\text{Be}$  ion beam. *Phys. Lett. B* **2022**, *824*, 136819. [[CrossRef](#)]
19. Rapagnani, D.; De Cesare, M.; Alfano, D.; Buompane, R.; Cantoni, S.; De Stefano Fumo, M.; Del Vecchio, A.; D’Onofrio, A.; Porzio, G.; Rufolo, G.; et al. Ion Beam Analysis for recession determination and composition estimate of Aerospace Thermal Protection System materials. *Nucl. Instrum. Methods Phys. Res. Sect. B Beam Interact. Mater. Atoms* **2020**, *467*, 53–57. [[CrossRef](#)]
20. De Cesare, M.; Savino, L.; Di Leva, A.; Rapagnani, D.; Del Vecchio, A.; D’Onofrio, A.; Gialanella, L. Gamma and infrared novel methodologies in Aerospace re-entry:  $\gamma$ -rays crystal efficiency by GEANT4 for TPS material recession assessment and simultaneous dual color infrared temperature determination. *Nucl. Instrum. Methods Phys. Res. Sect. B Beam Interact. Mater. Atoms* **2020**, *479*, 264–271. [[CrossRef](#)]
21. Brandi, F.; L’Abate, L.; Rapagnani, D.; Buompane, R.; di Leva, A.; Gialanella, L.; Gizzi, L.A. Optical and spectroscopic study of a supersonic flowing helium plasma: Energy transport in the afterglow. *Sci. Rep.* **2022**, *10*, 5087. [[CrossRef](#)]

22. Goasduff, A.; Santonocito, D.; Menegazzo, R.; Capra, S.; Pullia, A.; Raniero, W.; Rosso, D.; Toniolo, N.; Zago, L.; Naselli, E.; et al. A high resolution  $\gamma$ -ray array for the pandora plasma trap. *Front. Phys.* **2022**, *10*, 936081. [[CrossRef](#)]
23. Ciani, G.F.; Csedreki, L.; Balibrea-Correa, J.; Best, A.; Aliotta, M.; Barile, F.; Bemmerer, D.; Boeltzig, A.; Broggini, C.; Bruno, C.G.; et al. A new approach to monitor  $^{13}\text{C}$ -targets degradation in situ for  $^{13}\text{C}(\alpha, n)^{16}\text{O}$  cross-section measurements at LUNA. *Eur. Phys. J. A* **2020**, *56*, 75. [[CrossRef](#)]
24. Best, A.; Görres, J.; Junker, M.; Kratz, K.L.; Laubenstein, M.; Long, A.; Nisi, S.; Smith, K.; Wiescher, M. Low energy neutron background in deep underground laboratories. *Nucl. Instrum. Methods Phys. Res. Sect. A Accel. Spectrometers Detect. Assoc. Equip.* **2016**, *A812*, 1–6. [[CrossRef](#)]
25. Balibrea-Correa, J.; Ciani, G.; Buompane, R.; Cavanna, F.; Csedreki, L.; Depalo, R.; Ferraro, F.; Best, A. Improved pulse shape discrimination for high pressure  $^3\text{He}$  counters. *Nucl. Instrum. Methods Phys. Res. Sect. A Accel. Spectrometers Detect. Assoc. Equip.* **2018**, *906*, 103–109. [[CrossRef](#)]
26. Ananna, C.; Rapagnani, D.; Dell’Aquila, D.; Di Leva, A.; Imbriani, G.; Junker, M.; Mercogliano, D.; Best, A. Intrinsic background of EJ-309 liquid scintillator detectors. *Nucl. Instrum. Methods Phys. Res. Sect. A Accel. Spectrometers Detect. Assoc. Equip.* **2024**, *1060*, 169036. [[CrossRef](#)]

**Disclaimer/Publisher’s Note:** The statements, opinions and data contained in all publications are solely those of the individual author(s) and contributor(s) and not of MDPI and/or the editor(s). MDPI and/or the editor(s) disclaim responsibility for any injury to people or property resulting from any ideas, methods, instructions or products referred to in the content.